Internal Medicine
The Japanese Society of Internal Medicine
doi: 10.2169/internalmedicine.9465-22
Intern Med 61: 3361-3368, 2022
http://internmed.jp

【 CASE REPORT 】

Primary Hepatic Neuroendocrine Carcinoma with Thrombocytopenia Due to Diffuse Bone Marrow and Splenic Infiltration: An Autopsy Case

Shogo Nakano[1], Kosuke Minaga[1,2], Yasuhiro Tani[1], Kohei Tonomura[1], Yusuke Hanawa[1], Hiroki Morimura[1], Tomoko Terashita[1], Hisakazu Matsumoto[1], Hiroyoshi Iwagami[1], Yasuki Nakatani[1], Takuji Akamatsu[1], Yoshito Uenoyama[1], Chikara Maeda[3], Kazuo Ono[4], Tomohiro Watanabe[2] and Yukitaka Yamashita[1]

Abstract:
An 82-year-old man with fever and back pain was referred to our hospital and was thus found to be thrombocytopenic. A bone marrow biopsy revealed the diffuse infiltration of poorly differentiated neuroendocrine carcinoma (NEC). Computed tomography revealed a large hepatic mass. Considering the risk of bleeding due to thrombocytopenia, a needle biopsy was not performed. The patient rapidly deteriorated and died 10 days after presentation. An autopsy confirmed the diagnosis of primary hepatic NEC, with diffuse metastasis to the spleen, bone marrow, and systemic lymph nodes. This is an extremely rare case of NEC presenting with thrombocytopenia due to extensive bone marrow and splenic infiltration.

Key words: hepatic neuroendocrine carcinoma, neuroendocrine neoplasm, thrombocytopenia, bone marrow metastasis, disseminated carcinomatosis of the bone marrow

(Intern Med 61: 3361-3368, 2022)
(DOI: 10.2169/internalmedicine.9465-22)

Introduction

Neuroendocrine neoplasms (NENs) are a group of heterogeneous neoplasms that arise from the diffuse neuroendocrine cell system, and thus, NENs can develop in many different organs. Although the incidence and prevalence of NENs are thought to have increased over the past decades, the incidence of NENs is estimated to be around 7 cases per 100,000, which accounts for approximately 0.5% of all new malignancies (1, 2). The common primary organs of NENs are the gastrointestinal tract, lungs, and pancreas (1). Although the liver is the most common metastatic site of NENs, primary hepatic NENs are exceedingly rare, accounting for only 0.3-0.8% of all NENs (2, 3). Thus, the diagnosis of primary hepatic NENs should exclude metastasized NENs after careful consideration of all clinical and radiological information. According to the World Health Organization (WHO) classification (5th edition), NENs are classified based on the degree of tumor cell differentiation, as follows: well-differentiated neuroendocrine tumor, poorly differentiated neuroendocrine carcinoma (NEC), and mixed neuroendocrine-non-neuroendocrine neoplasm (MiNEN) (4). Among NENs, patients with NEC tend to have a poor prognosis because most already have lymph node or distant metastases at the time of diagnosis. However, NEC cases with diffuse bone marrow (BM) involvement at the initial diagnosis are extremely rare (5-8). We herein report an autopsy case of primary hepatic NEC (PHNEC) with extensive BM and splenic infiltration causing thrombocytopenia.

[1]Department of Gastroenterology, Japan Red Cross Wakayama Medical Center, Japan, [2]Department of Gastroenterology and Hepatology, Kindai University Faculty of Medicine, Japan, [3]Department of Radiology, Japan Red Cross Wakayama Medical Center, Japan and [4]Department of Pathology, Japan Red Cross Wakayama Medical Center, Japan
Received: January 25, 2022; Accepted: February 23, 2022; Advance Publication by J-STAGE: April 9, 2022
Correspondence to Kosuke Minaga, kousukeminaga@med.kindai.ac.jp

Table. Summary of the Laboratory Data.

Hematology	
White blood cells	9,900 /μL
Neutrophil	66.7 %
Monocyte	10.9 %
Lymphocyte	19.8 %
Red blood cells	325×10^4 /μL
Hemoglobin	10.9 g/dL
Platelets	3.3×10^4 /μL
Blood chemistry	
Total protein	7.8 g/dL
Albumin	3.8 g/dL
Aspartate aminotransferase	168 U/L
Alanine aminotransferase	42 U/L
Lactate dehydrogenase	1,454 U/L
Alkaline phosphatase	342 U/L
γ-glutamyl transpeptidase	147 U/L
Total-bilirubin	1.2 mg/dL
Uric acid	9.4 mg/dL
Blood-urea-nitrogen	37 mg/dL
Creatinine	1.43 mg/dL
C-reactive protein	9.1 mg/dL
Ferritin	5,882 ng/mL
Hemoglobin A1c	7.0 %
Coagulation	
PT-INR	0.99
APTT	35.7 s
D-dimer	21.8 μg/mL
Fibrinogen	347 mg/dL
Tumor marker	
AFP	9.7 ng/mL
PIVKA-II	43 mAU/mL
CEA	2.5 ng/mL
CA19-9	28.1 U/mL
NSE	467 ng/mL
ProGRP	73.3 pg/mL
sIL2-R	1,887 U/mL

PT-INR: prothrombin time-international normalized ratio, APTT: activated partial thromboplastin time, AFP: alpha-fetoprotein, PIVKA-II: protein induced by vitamin K absence or antagonist II, CEA: carcinoembryonic antigen, CA19-9: carbohydrate antigen 19-9, NSE: neuron-specific enolase, ProGRP: pro-gastrin releasing peptide, sIL2-R: soluble interleukin-2 receptor

Case Report

An 82-year-old Japanese male presented with intermittent fever and progressive back pain over a 2-week period. This was associated with loss of appetite and weight loss. He had a medical history of type 2 diabetes that had been well-controlled with oral medication (latest hemoglobin A1c: 7.0%). He was a non-smoker and a non-drinker without obesity.

He was admitted to our hospital for further evaluation. His vital signs were as follows: body temperature: 37.5°C, blood pressure: 125/61 mmHg, pulse rate: 92 beats/min, respiratory rate: 20/min, and oxygen saturation: 95% on room air. Physical examination revealed no specific abnormalities. The laboratory findings are summarized in Table. A complete blood count showed severe thrombocytopenia (platelet count: 3.3×10^4/μL) alongside coagulopathy with marked elevated level of D-dimer (21.8 μg/mL). A serum biochemistry analysis revealed a marked elevation of lactic dehydrogenase (LDH; 1,454 U/L), ferritin (5,882 ng/mL; reference range: 40-465 ng/mL), and soluble interleukin-2 receptor (1,887 U/mL; reference range: 122-496 U/mL). In addition, the C-reactive protein level was elevated (9.1 mg/dL). As for tumor markers, the levels of alpha-fetoprotein (AFP), carcinoembryonic antigen, and carbohydrate antigen 19-9 were within the normal limits, whereas the level of neuron-specific enolase (NSE; 467 ng/mL; normal value: <16.2 ng/mL) was significantly high. The patient was found to be positive for hepatitis C virus (HCV) by antibody testing, but he was negative for quantitative HCV-(RNA) testing.

The patient's intermittent fever, thrombocytopenia, and markedly elevated serum LDH and ferritin levels led us to suspect either hemophagocytic syndrome or hematologic malignancies. A BM smear revealed a decrease in normal hematopoietic elements and a significant increase in immature blastic cells with a high nuclear-to-cytoplasmic ratio (Fig. 1). The cells had a high mitotic index (>20/high power field) and there were small aggregates of necrotic tumor cells. Immunohistochemistry of the samples obtained by a BM biopsy showed tumor cells that were positive for synaptophysin, NSE, and membranous staining CD56 (Fig. 2). Chromogranin A, cytokeratin AE1/AE3, CD45, and thyroid transcription factor 1 were all negative on immunohistochemical staining. The findings on pathology and immunohistochemistry suggested BM metastatic carcinoma with neuroendocrine differentiation.

Computed tomography (CT) and magnetic resonance imaging (MRI) showed a large hepatic mass in the right lobe measuring 60×55 mm in size. The lesion was of low-density with a round shape and unclear borders on unenhanced CT. In contrast-enhanced CT, the lesion showed hypo-enhancement in the delayed phase (Fig. 3). Furthermore, CT also revealed multiple hepatic hilar and para-aortic lymphadenopathies and splenomegaly. The CT density of BM was diffusely high, suggesting the possibility of disease involvement (Fig. 3). On MRI, the lesion showed a low signal intensity on T1-weighted images and high signal intensity on T2-weighted and diffusion-weighted images (Fig. 4). Dynamic contrast-enhanced MRI using gadolinium-ethoxybenzyl-diethylenetriamine pentaacetic acid showed heterogeneous hypo-enhancement patterns in all phases (Fig. 4). In addition, the BM showed high signal intensity on diffusion-weighted images (Fig. 4).

Although PHNEC with BM metastasis was suspected based on the findings of imaging and a BM biopsy, a needle biopsy for the hepatic mass was not performed due to the low platelet levels and risk of coagulopathy. Moreover, chemotherapy could not be administered because his condition

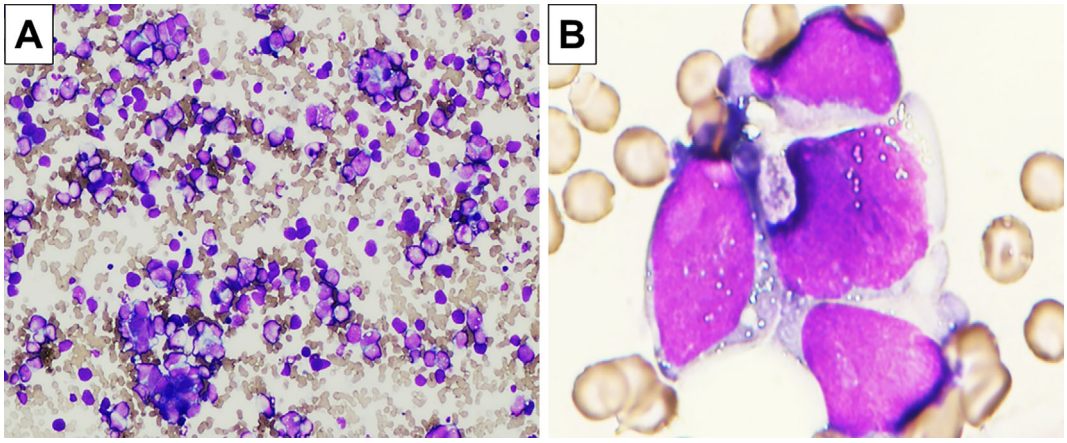

Figure 1. **The findings of a bone marrow aspiration sample (A, B). A bone marrow smear showing a decrease in normal hematopoietic elements and a significant increase in immature blastic cells with a high nuclear-to-cytoplasmic ratio (May-Giemsa staining). Magnification: A, ×100; B, ×1,000.**

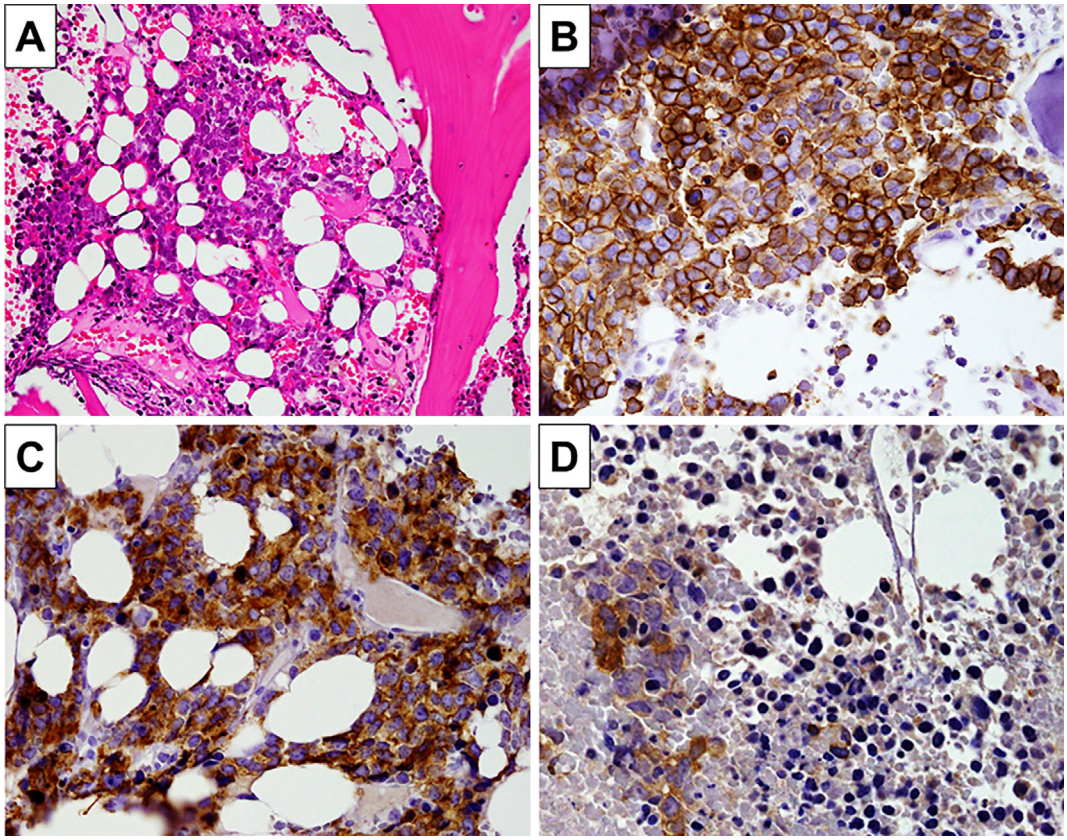

Figure 2. **A pathological analysis of the bone marrow biopsy sample obtained from the left Ilium. Numerous small round cells with scanty cytoplasm are shown (Hematoxylin and Eosin staining) (A). An immunohistochemical analysis showing tumor cells positive for CD56 (B), synaptophysin (C), and neuron-specific enolase (D). Magnification: A, ×200; B-D, ×400.**

had rapidly deteriorated. Due to this poor clinical condition, the patient was given a DNAR (do not attempt resuscitation) order and passed away 10 days after admission. The patient's family gave their consent for an autopsy, which was performed 5 hours after death.

On autopsy, the liver size was normal (1,238 g) with a smooth surface. A 10 cm×5 cm×5 cm mass with well-defined borders was found in the right lobe of the liver. On microscopic review, the tumor was composed of small, round, eosinophilic cells with hyperchromatic nuclei and scanty cytoplasm. Many foci of tumor necrosis were identified within the lesion. The findings on immunohistochemical staining were completely consistent with those of BM biopsy samples (Fig. 5). The Ki-67 labeling index of the tumor cells was 70%. The results of CK7, CK20, and HepPar1 staining of the hepatic tumor cells were negative. The lesion

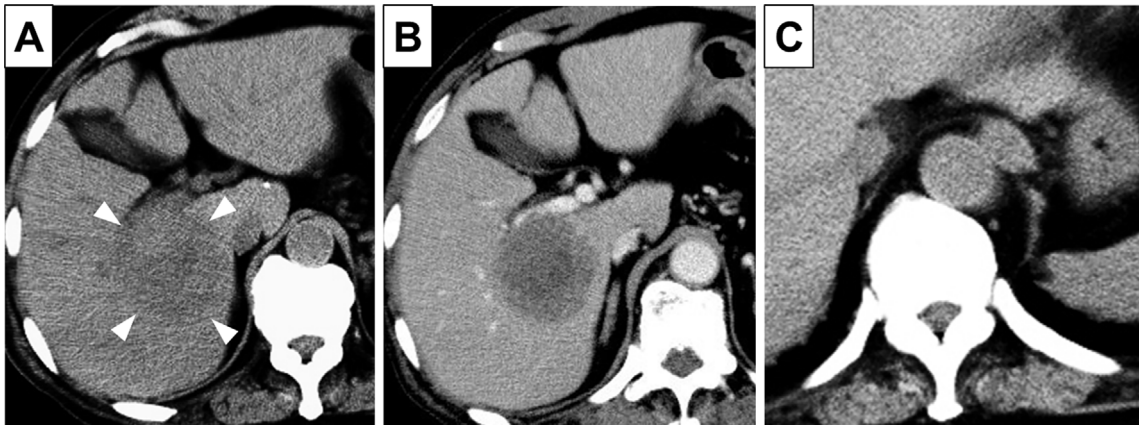

Figure 3. **Unenhanced computed tomography (CT) showing a large hepatic mass in the right lobe measuring 60×55 mm in size with low-density, a round shape, and unclear borders (A). Contrast-enhanced CT showing hypo-enhancement of the lesion in the delayed phase (B). The bone marrow was hyperdense on unenhanced CT (C).**

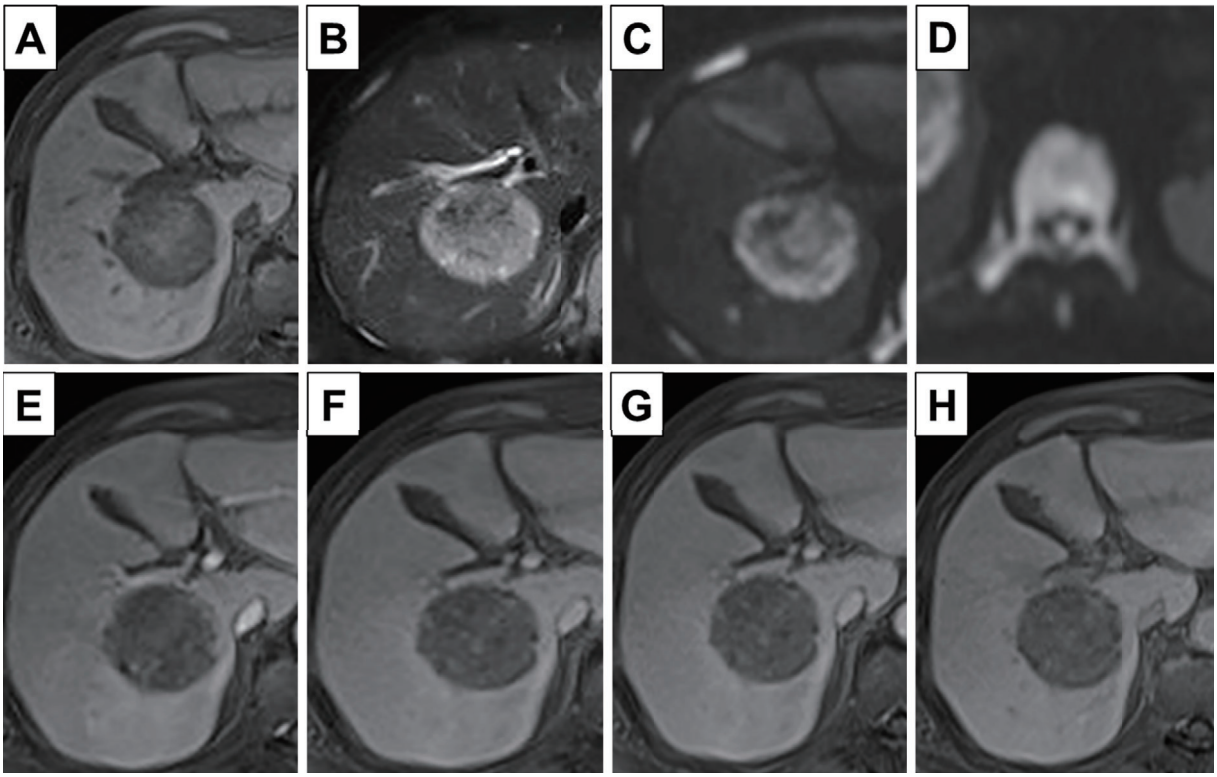

Figure 4. **Magnetic resonance imaging (MRI) showing the hepatic mass in the right lobe with low signal intensity on T1-weighted images and high signal intensity on fat-saturated T2-weighted and diffusion-weighted images (A-C). Dynamic contrast-enhanced MRI using gadolinium-ethoxybenzyl-diethylenetriamine pentaacetic acid showing heterogeneous hypo-enhancement patterns in all four phases: arterial phase (E), portal phase (F), delayed phase (G), hepatobiliary phase (H). The bone marrow showing a high signal intensity on diffusion-weighted MRI (D).**

was classified as a small-cell-type NEC. In addition, the liver showed small-sized round tumor cells diffusely infiltrating the sinusoids of the entire liver without forming a mass (Fig. 5). The surrounding liver parenchyma had non-cirrhotic foci (A1, F2, based on the new Inuyama classification). Similar sinusoidal infiltration of tumor cells was observed in the spleen. The BM obtained from the ribs and L3 showed hypo-cellular hematopoiesis with diffuse tumor cell involvement (Fig. 6). Numerous lymph node metastases were noted at the para-aortic, para-pancreatic, periportal, and mediastinal lymph nodes. There were no other candidates for a primary lesion except the liver. In particular, although

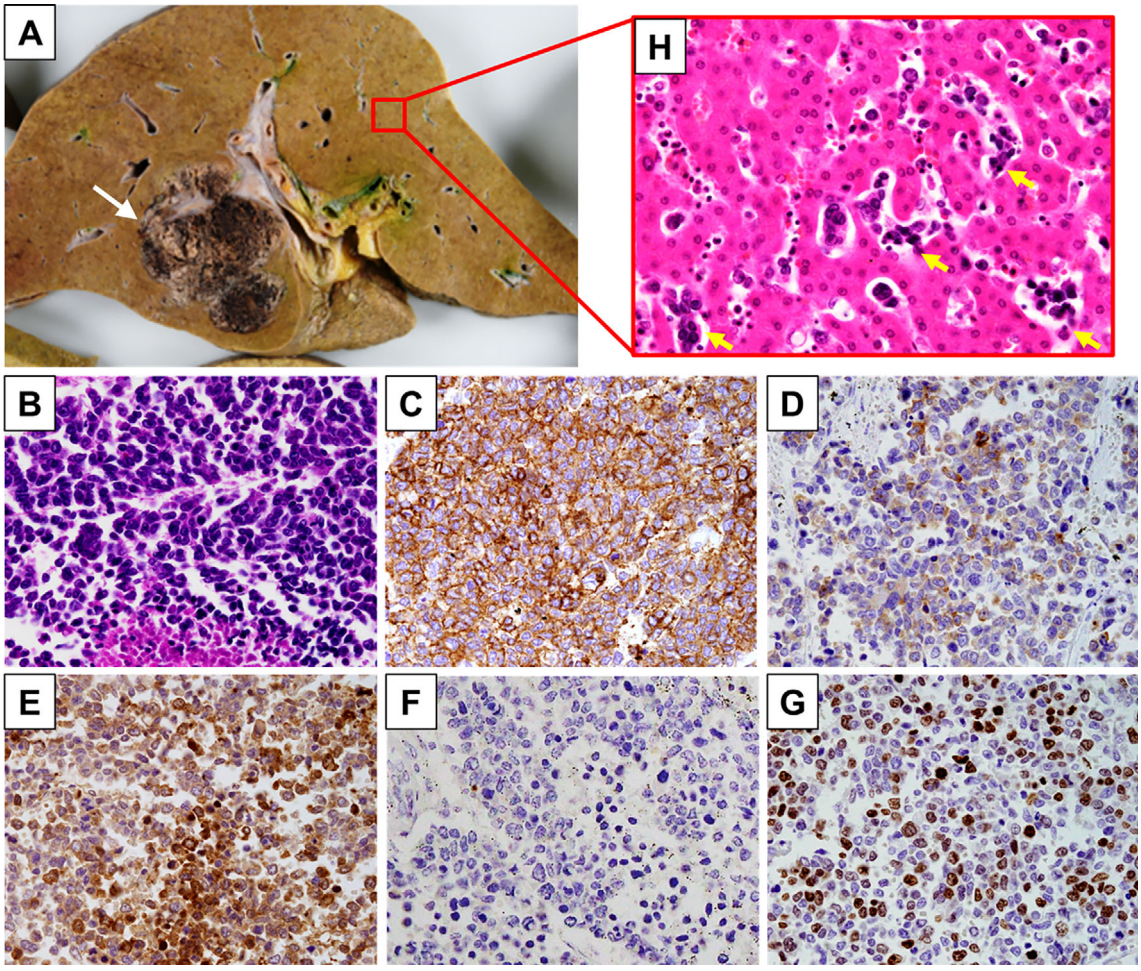

Figure 5. **Pathological anatomical findings of the liver obtained during autopsy. Cut surface of the liver showing a large tumor with necrotic foci in the right lobe (arrow) (macroscopic finding) (A). Microscopic findings of the liver mass showing tumor cells composed of small-sized round cells with hyperchromatic nuclei and scanty cytoplasm (B-G). An immunohistochemical analysis showing tumor cells to be positive for CD56 (C), synaptophysin (D), and neuron-specific enolase (E), and negative for HepPar1 (F). Tumor cells demonstrating a Ki-67 labeling index of 70% (G). Diffuse sinusoidal infiltration by small-sized round tumor cells (arrows) throughout the liver (H). Magnification: B-H, ×400.**

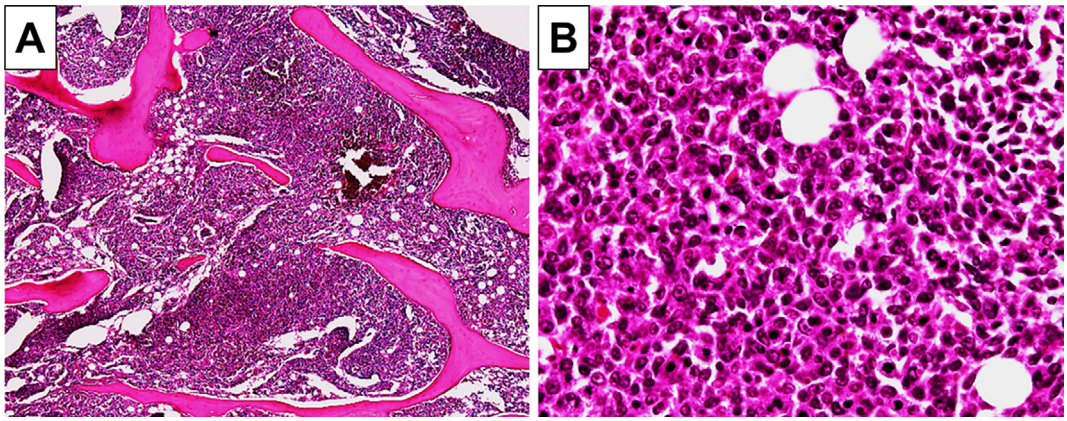

Figure 6. **Pathological findings of a bone marrow specimen taken from the lumbar spine during autopsy (Hematoxylin and Eosin staining). The bone marrow with a cell density of >90% (A). Diffuse infiltration of small round tumor cells with almost no normal hematopoietic cells (B). Magnification: A, ×40; B, ×400.**

the gastrointestinal tract is a frequent site of primary NEC, an endoscopic examination could not be performed due to the patient's poor general condition. Therefore, the gastrointestinal tract was thoroughly examined during autopsy; however, no lesions with suspected NEC were found. Based on these autopsy findings, the final diagnosis was small-cell-type PHNEC with metastasis to the spleen, BM, and systemic lymph nodes. The cause of death was thus deemed to be multiple organ failure due to extensive neoplastic involvement.

Discussion

We encountered an extremely rare case of PHNEC presenting with thrombocytopenia which was associated with diffuse BM involvement and sinusoidal infiltration in the hepatic and splenic parenchyma.

Although BM is an infrequent metastatic site of solid tumors, diffuse BM involvement (also known as disseminated carcinomatosis of the BM) is associated with a poor prognosis and significant morbidity (9). The incidence of BM metastasis varies across tumor types. BM metastasis from non-hematologic solid malignancies is especially common in gastric, prostate, and breast cancers (9-11). This condition can result in impaired hematopoiesis. Particularly, anemia and thrombocytopenia are usually the first clinical symptoms in patients with carcinomatosis of the BM (9, 11). Indeed, in the present case, during the work-up for thrombocytopenia, disseminated carcinomatosis of the BM was diagnosed on a BM biopsy. Since BM involvement is extremely rare in NEC, not much is known regarding the epidemiology, treatment, and outcomes of NEC patients affected with BM metastasis (5-8). Notably, the entire BM in this patient was hyperdense on CT and hyperintense on diffusion-weighted MRI, thus suggesting diffuse BM involvement of the malignancy. Only one case of PHNEC with BM metastasis has previously been reported (12). The case was a young human immunodeficiency virus-positive patient who presented with pancytopenia, hepatic failure, and coagulopathy who died only a few hours after admission due to multiorgan failure (12). In that case, distinct hepatomegaly was observed without the formation of a mass. Diffuse sinusoidal infiltration by NEC cells throughout the enlarged liver was also observed by autopsy. This diffuse infiltration of NEC cells in the sinusoidal space in the liver parenchyma is a characteristic feature of PHNEC that presents with hepatomegaly without forming a mass which rapidly progresses to acute liver failure (13). Similarly, in our case, although hepatomegaly was not observed, the diffuse sinusoidal infiltration of tumor cells was observed throughout the liver, including a sinusoidal space far from the primary lesion. Interestingly, extensive sinusoidal infiltration without mass formation was also observed in the spleen. Our case exhibited a unique development pattern of PHNEC presenting with diffuse BM infiltration and diffuse sinusoidal infiltration in both the hepatic and splenic parenchyma.

The clinical diagnosis of PHNEC remains challenging because of its rarity and non-specific laboratory and radiological findings. Serum liver tests are mostly in the normal range and circulating tumor markers have no diagnostic value (14). PHNEC should be distinguished from more frequent hepatic malignancies such as hepatocellular carcinoma (HCC) and cholangiocarcinoma. HCC often accompanies chronic hepatitis and cirrhosis, and most patients have elevated serum AFP levels. In addition, HCCs typically demonstrate contrast agent filling in the arterial phase but then are washed-out in the venous phase. This case had atypical findings for HCC because the serum AFP level was normal, and on contrast-enhanced MRI, the lesion showed hypo-enhancement in both arterial and venous phases. Regarding the radiological findings of PHNEC, previous studies have shown that PHNEC appears as a low-density mass with an uneven or annular enhancement at the peripheral margin in the arterial phase and consistent or declined enhancement in the venous phase (15-17). The center of the mass is sometimes not enhanced, signifying tumor necrosis or hemorrhaging (15). On T2-weighted and diffusion-weighted MRI, PHNEC is often well-circumscribed, lobulated, or with multiple hyperintense nodular masses. On T1-weighted MRI, these masses are well-circumscribed, heterogeneous, and hypointense (18). Despite these characteristics on imaging, it seems difficult to distinguish PHNEC from cholangiocarcinoma, liver metastasis, and poorly differentiated HCC. Since the radiological and laboratory findings of PHNECs are not specific, a pathological evaluation is needed to make a definitive diagnosis. Therefore, despite the risk of needle tract seeding, a needle biopsy for such hepatic masses is needed to accurately diagnose PHNEC. On pathological examination, immunohistochemical staining with pan-neuroendocrine markers such as chromogranin A, synaptophysin, CD56, and NSE should be performed whenever there is a morphological suspicion of neuroendocrine differentiation.

One major question in this case is what cells PHNEC originated from. Currently, two hypotheses have been proposed for the origin of PHNECs (19-21). First, PHNECs originate from stem cells that differentiated from other malignant hepatic cells and thereafter are converted into neuroendocrine cells. This hypothesis is supported by several case reports of MiNENs with both HCC and NEC components (22-24). The majority of these composite tumors are accompanied by chronic hepatitis or liver cirrhosis (24). Moreover, a recent study showed that PHNEC and HCC have shared the same molecular and genetic features (25). In our case, although serum HCV tests suggested a previous HCV infection with spontaneous resolution and mild chronic hepatitis was observed on autopsy, the patient neither had a history of liver dysfunction nor did he have cirrhosis. Furthermore, autopsy revealed no HCC-related components in the liver tumor. Therefore, it seems difficult to presume that the PHNEC originated from stem cells which differentiated from other malignant hepatic cells. Another hypothesis regarding the origin of PHNECs is that neuroendocrine cells

in the intrahepatic bile duct epithelium undergo malignant conversion and thereafter become PHNECs (19). Unfortunately, little is known about the molecular pathogenetic pathways underlying the development of PHNEC due to their rarity (26, 27). Although the exact origin of PHNEC is uncertain due to the lack of genetic and molecular analyses, the latter hypothesis seems to be more favorable in the present case because of the formation of a single large hepatic mass without other tumor components aside from neuroendocrine differentiation.

Based on limited evidence, the current gold standard of treatment for PHNEC is radical surgical resection with platinum-based chemotherapy or transcatheter arterial chemoembolization (28, 29). However, the rate of recurrence and hematogenous or lymphatic metastasis after surgical resection for PHNEC is extremely high, and the prognosis is poor (29). Park et al. reported the median overall survival in 12 reported PHNEC cases to be 16.5 months (29). Recently, a literature review of case studies showed the 5-year survival rate of 33 PHNEC cases to be poor (9.1%) (30). Chen et al. reported that a high expression of Ki-67 was an independent prognostic factor for primary hepatic NENs (14). In the present case, radical resection could not done due to the presence of BM metastasis at the time of diagnosis, and the Ki-67 index was as high as 70%, thus suggesting a poor prognosis. In addition, chemotherapy could not be introduced due to the rapid deterioration of the patient's general condition. However, palliative chemotherapy is recommended if it can be tolerated.

In conclusion, the patient in this case report had advanced-stage PHNEC with a fatal outcome. To the best of our knowledge, this is the second case report of PHNEC with diffuse BM and splenic infiltration causing thrombocytopenia. This case supports the importance of performing an aggressive BM biopsy for the diagnosis of disseminated carcinomatosis of the BM caused by nonhematologic malignancies.

The authors state that they have no Conflict of Interest (COI).

References

1. Dasari A, Shen C, Halperin D, et al. Trends in the incidence, prevalence, and survival outcomes in patients with neuroendocrine tumors in the United States. JAMA Oncol **3**: 1335-1342, 2017.
2. Nomura Y, Nakashima O, Akiba J, et al. Clinicopathological features of neoplasms with neuroendocrine differentiation occurring in the liver. J Clin Pathol **70**: 563-570, 2017.
3. Yao JC, Hassan M, Phan A, et al. One hundred years after "carcinoid": epidemiology of and prognostic factors for neuroendocrine tumors in 35,825 cases in the United States. J Clin Oncol **26**: 3063-3072, 2008.
4. Klimstra DS, Klöppel G, La Rossa S, Rindi G. Classification of neuroendocrine neoplasms of the digestive system. In: WHO Classification of Tumors Digestive System Tumors. 5th ed. International Agency for Research on Cancer (IARC), Lyon, 2019: 16-19.
5. Hsia CC, Chin-Yee IH. Metastatic neuroendocrine cells. Blood **118**: 2387, 2011.
6. Helbig G, Straczyńska-Niemiec A, Szewczyk I, Nowicka E, Bierzyńska-Macyszyn G, Kyrcz-Krzemień S. Unexpected cause of anemia: metastasis of neuroendocrine tumor to the bone marrow. Pol Arch Med Wewn **124**: 635-636, 2014.
7. Salathiel I, Wang C. Bone marrow infiltrate by a poorly differentiated neuroendocrine carcinoma. Pathol Res Pract **199**: 483-486, 2003.
8. Kawashima I, Fukasawa H, Kasai K, et al. Bone marrow invasion of small cell neuroendocrine carcinoma of the endometrium: a diagnostic pitfall mimicking a haematological malignancy. Intern Med **58**: 2561-2568, 2019.
9. Ozkalemkas F, Ali R, Ozkocaman V, et al. The bone marrow aspirate and biopsy in the diagnosis of unsuspected nonhematologic malignancy: a clinical study of 19 cases. BMC Cancer **5**: 144, 2005.
10. Delsol G, Guiu-Godfrin B, Guiu M, Pris J, Corberand J, Fabre J. Leukoerythroblastosis and cancer frequency, prognosis, and physiopathologic significance. Cancer **44**: 1009-1013, 1979.
11. Kopp HG, Krauss K, Fehm T, et al. Symptomatic bone marrow involvement in breast cancer-clinical presentation, treatment, and prognosis: a single institution review of 22 cases. Anticancer Res **31**: 4025-4030, 2011.
12. Byers JT, Mendoza A, Wu D, Kahlon JS, Qing X, French SW. Case report: an HIV+ patient presenting with pancytopenia, hepatic failure, and coagulopathy; a rare small cell liver carcinoma with diffuse splenic and bone marrow metastasis diagnosed at autopsy. Exp Mol Pathol **103**: 178-180, 2017.
13. Lo AA, Lo EC, Li H, et al. Unique morphologic and clinical features of liver predominant/primary small cell carcinoma-autopsy and biopsy case series. Ann Diagn Pathol **18**: 151-156, 2014.
14. Chen RW, Qiu MJ, Chen Y, et al. Analysis of the clinicopathological features and prognostic factors of primary hepatic neuroendocrine tumors. Oncol Lett **15**: 8604-8610, 2018.
15. Chen Z, Xiao HE, Ramchandra P, Huang HJ. Imaging and pathological features of primary hepatic neuroendocrine carcinoma: an analysis of nine cases and review of the literature. Oncol Lett **7**: 956-962, 2014.
16. Han Y, Li L, Sun H. Computed tomography and magnetic resonance imaging in the diagnosis of primary neuroendocrine tumors of the liver. World Neurosurg **138**: 723-731, 2020.
17. Huang YQ, Xu F, Yang JM, Huang B. Primary hepatic neuroendocrine carcinoma: clinical analysis of 11 cases. Hepatobiliary Pancreat Dis Int **9**: 44-48, 2010.
18. Yang K, Cheng YS, Yang JJ, Jiang X, Guo JX. Primary hepatic neuroendocrine tumors: multi-modal imaging features with pathological correlations. Cancer Imaging **17**: 20, 2017.
19. Pilichowska M, Kimura N, Ouchi A, Lin H, Mizuno Y, Nagura H. Primary hepatic carcinoid and neuroendocrine carcinoma: clinicopathological and immunohistochemical study of five cases. Pathol Int **49**: 318-324, 1999.
20. Gravante G, De Liguori Carino N, Overton J, Manzia TM, Orlando G. Primary carcinoids of the liver: a review of symptoms, diagnosis and treatments. Dig Surg **25**: 364-368, 2008.
21. Gould VE, Banner BF, Baerwaldt M. Neuroendocrine neoplasms in unusual primary sites. Diagn Histopathol **4**: 263-277, 1981.
22. Nishino H, Hatano E, Seo S, et al. Histological features of mixed neuroendocrine carcinoma and hepatocellular carcinoma in the liver: a case report and literature review. Clin J Gastroenterol **9**: 272-279, 2016.
23. Lan J, Guo D, Qin X, Chen B, Liu Q. Mixed neuroendocrine carcinoma and hepatocellular carcinoma: a case report and literature review. Front Surg **8**: 678853, 2021.
24. Nakano A, Hirabayashi K, Yamamuro H, et al. Combined primary hepatic neuroendocrine carcinoma and hepatocellular carcinoma: case report and literature review. World J Surg Oncol **19**: 78, 2021.

25. Shi C, Jug R, Bean SM, Jeck WR, Guy CD. Primary hepatic neoplasms arising in cirrhotic livers can have a variable spectrum of neuroendocrine differentiation. Hum Pathol **116**: 63-72, 2021.
26. Rasmussen JØ, von Holstein SL, Prause JU, et al. Genetic analysis of an orbital metastasis from a primary hepatic neuroendocrine carcinoma. Oncol Rep **32**: 1447-1450, 2014.
27. Pastrián LG, Ruz-Caracuel I, Gonzalez RS. Giant primary neuroendocrine neoplasms of the liver: report of 2 cases with molecular characterization. Int J Surg Pathol **27**: 893-899, 2019.
28. Li S, Niu M, Deng W, et al. Efficacy of chemotherapy versus transcatheter arterial chemoembolization in patients with advanced primary hepatic neuroendocrine carcinoma and an analysis of the prognostic factors: a retrospective study. Cancer Manag Res **13**: 9085-9093, 2021.
29. Park CH, Chung JW, Jang SJ, et al. Clinical features and outcomes of primary hepatic neuroendocrine carcinomas. J Gastroenterol Hepatol **27**: 1306-1311, 2012.
30. Seki Y, Sakata H, Uekusa T, et al. Primary hepatic neuroendocrine carcinoma diagnosed by needle biopsy: a case report. Surg Case Rep **7**: 236, 2021.